Role of pH and Crosslinking Ions on Cell Viability and Metabolic Activity in Alginate-gelatin 3D Prints

Andrea Souza , Matthew Parnell , Brian J. Rodriguez , Emmanuel Reynaud *

Posted Date: 15 September 2023

doi: 10.20944/preprints202309.1086.v1

Keywords: 3D printing; alginate-gelatin hydrogel; pH; CaCl2; BaCl2; U2OS; NIH/3T3; fluid-phase

Article

Role of pH and Crosslinking Ions on Cell Viability and Metabolic Activity in Alginate-Gelatin 3D Prints

Authors: Souza Andrea [1], Parnell Matthew [1], Rodriguez Brian J. [2] and Reynaud Emmanuel G. [1,*]

[1] School of Biomolecular and Biomedical Science, University College Dublin, Belfield, Dublin 4, Ireland;
[2] School of Physics, University College Dublin, Belfield, Dublin 4, Ireland
* Correspondence: emmanuel.reynaud@ucd.ie

Abstract: Alginate-gelatin hydrogels are extensively used in bioengineering. However, despite different formulations being utilized for growing different cell types *in vitro*, their pH and its effect, together with the crosslinking ions, of those formulations are still infrequently assessed. In this work we studied how these elements can affect hydrogel stability and printability and influence U2OS and NIH/3T3 cell viability and metabolism on the resulting 3D prints. In this context, 6% alginate + 2% gelatin hydrogels were prepared with 0.1 M MES buffer with pH 5.5, 6.5, 7.0 or 8.0, printed by extrusion-based 3D printing, and crosslinked immediately after printing with either $CaCl_2$ or $BaCl_2$. Our results showed that both the buffer pH and the crosslinking ion (Ca^{2+} or Ba^{2+}) influence the swelling and degradation rates of the prints. Moreover, the buffer pH influenced the printability of the hydrogel in air, but when printed directly in a fluid-phase $CaCl_2$ or $BaCl_2$ crosslinking bath. In addition, both U2OS and NIH/3T3 cells showed greater cell metabolic activity on one-layer prints crosslinked with Ca^{2+}. Besides, Ba^{2+} increased cell death of NIH/3T3 cells while had no effect on the U2OS cell viability. The pH of the buffer also caused an important impact on the cell behaviour. U2OS cells showed a 2.25-fold cell metabolism increase on one-layer prints prepared at pH 8.0 in comparison to those prepared at pH 5.5. Whereas, NIH/3T3 cells showed greater metabolism on one-layer prints with pH 7.0. Finally, we observed a difference on cell arrangement of the U2OS cells growing on prints prepared from hydrogels with acidic buffer in comparison to cells growing on those prepared using neutral or basic buffer. These results show that both pH and crosslinking ion influence hydrogel strength and cell behaviour.

Keywords: 3D printing; alginate-gelatin hydrogel; pH; $CaCl_2$; $BaCl_2$; U2OS; NIH/3T3; fluid-phase

1. Introduction

Recently, the 3D (bio)printing technology has shown its potential in replacing and complementing existing methods in basic research, drug delivery and screening, and medical procedures. For instance, it allows the production of bioprinted full skin equivalent and it can support bone and capillary formation, breast fat tissue growth, among other biological structures created in (bio)printed scaffolds *in vitro* [1–4]. However, even though some important advances have been made to date, this technology is still evolving and in need of more research over the basic requirements needed to create optimal matrices for growing tissues *in vitro*. To construct a successful environment, the biological, physical, mechanical, and chemical aspects of the scaffolds should be established specifically to each tissue and/or purpose of the study as pathologic tissues behave differently from healthy ones.

Hydrogels are largely used in the bioengineering field due to their ability to mimic the extracellular environment. Alginate hydrogel is the second most used natural bioink in this field because of its biocompatibility, biomimetic, tunability, good printability, and crosslinkability characteristics [5]. However, alginate's highly swollen polymer crosslinked network can lead to instability and degradation just a few days under cell culture conditions [6]. Therefore, tailoring the alginate into a more biomimetic matrix will make it a more attractive biomaterial. The addition of gelatin can improve the mechanical properties of the hydrogel increasing its elasticity and decreasing its stiffness [7,8]. Moreover, Alsberg *et al* (2001) has shown that the incorporation of RGD molecules into alginate gels transform the hydrogel in a suitable matrix to promote bone formation [9]. Finally,

 doi:10.20944/preprints202309.1086.v1

an additional way to tailor its mechanical properties is the degree of the crosslinking which can be determine by the crosslinker type, concentration, temperature, time of exposure, etc [10,11].

Alginate can be chemically or physically crosslinked. Chemical crosslinking involves the formation of irreversible covalent bonds between alginate chains and leading in general to better stability under cell culture conditions [12–15]. Whereas physical crosslinking involves hydrogen bonding, hydrophobic bonding, ionic bonding, electrostatic interactions, etc and create reversible three-dimensional structures [13–16]. Alginate is usually ionically crosslinked in the bioengineering field by divalent cations in particular calcium. However, the Ca^{2+} molecules from the crosslinked hydrogel can be released to the medium causing inflammatory responses *in vitro* and *in vivo* [17]. Another possibility of ionic crosslinking of alginate substrates for cell-based therapies is the use of Ba^{2+} molecules. Barium has better affinity to alginate, therefore provides hydrogels with stronger mechanical properties and increased young's modulus in comparison to calcium [18]. Yet Ba^{2+} has shown diverse effect on cell viability and proliferation depending on the cell type. For instance, Luca *et al* (2007) reported that encapsulated Sertoli cells in alginate microbeads showed greater viability after barium crosslinking in comparison to calcium [19]. Whereas Mores *et al* (2015) showed a decrease of mononuclear phagocyte viability caused by apoptosis due to barium crosslinking [20]. Therefore, as few studies about barium crosslinking are available in the literature, the alginate crosslinking with barium should be studied carefully for each cell type and condition.

Another important aspect during the preparation of hydrogel scaffolds for bioengineering is the pH of the solution. FitzSimons *et al* (2022) described that the pH influences the polymers bonding kinetics, the mechanical properties, and the protein release of PEG hydrogels crosslinked via reversible thia-Michael addition [21]. Besides, the pH is involved in regulating the solubility of alginate/gelatin in aqueous phase [22]. Bouhadir *et al* (2001) showed that increasing the pH leads to an increase of the alginate hydrogel degradability [23]. In addition, the alginate hydrogels viscosity increases with the decrease of the pH reaching to a maximum viscosity at pH 3.0 – 3.5 once the carboxylate groups present in the alginate chain protonate and form hydrogen bonds [15]. Recently the effect of pH on hydrogels has been largely studied specially regarding the production of responsive hydrogels used to deliver drugs or optimize cell growth and differentiation. Tailoring the hydrogel's mechanical properties, degradation rate, and affinity to proteins via pH changes is a costless and important tool for the bioengineering field. Therefore, understanding the effect of the hydrogel's intrinsic pH as well as the surrounding pH on the hydrogel's mechanics and kinetics is fundamental to control accurately the hydrogel behaviour.

In this work we used a hydrogel composed of 6% alginate and 2% gelatin (w/v) to investigate the impact of different pH values (5.5, 6.5, 7.0, 8.0) and crosslinking ions ($CaCl_2$, $BaCl_2$) on the hydrogel stability under cell culture conditions incubated with either DMEM or RPMI 1640. The two media are widely used in cell culture and present differences in their composition regarding calcium (RPMI: 0.8 mM, DMEM: 1.8 mM) and phosphate (RPMI: 5 mM, DMEM: 1 mM) concentrations [24]. Whereas, both media present physiological pH 7.0 – 7.4. The printability of the alginate-gelatin hydrogel with different pH values were tested in air and under fluid-phase using a support bath containing either 100 mM $CaCl_2$ or 100 mM $BaCl_2$. Air printing allows the printability of high viscosity biomaterials and bioinks while the fluid phase printing allows the printability of low viscosity biomaterials and bioinks [25]. Finally, to broaden our understanding, different cell types (the human osteosarcoma cell line U2OS and the murine fibroblast cell line NIH/3T3) were used to study the effect of the substrate's pH (as modified by buffer) and crosslinking on cell viability and metabolism.

2. Materials and methods

2.1. Materials

Alginic acid sodium salt type 1, Sodium Chloride, Calcium Chloride, and EDC (1-ethyl-3-(3-dimethylaminopropyl) carbodiimide hydrochloride) were purchased from Thermo Fisher Scientific; gelatin type B: bovine skin, was purchased from Sigma-Aldrich; MES buffer pH 5.5, 6.5, 7.0, and 8.0, Polyetherimide (PEI), Barium Chloride, and NHS (N-hydroxysuccinimide) were purchased from

Preprints (www.preprints.org) | NOT PEER-REVIEWED | Posted: 15 September 2023 doi:10.20944/preprints202309.1086.v1

Alfa Aesar; MVG GRGDSP (RGD) was purchased from Novatech, RPMI 1640, DMEM, fetal bovine serum (FBS), and trypsin/ EDTA were purchased from Gibco Life Technologies. U2OS human osteosarcoma cell line (ATCC® HTB-96™) and NIH/3T3 murine fibroblast cell line (ATCC® CRL-1658™) were used as cell models.

2.2. Methods

2.2.1. Cell Culture

U2OS cells and NIH/3T3 cells were cultured in 75cm^2 flasks in complete RPMI 1640 and DMEM, respectively, both supplemented with 10% FBS under a saturating humidified atmosphere at 37°C and 5% CO_2. Subconfluent cultures were passaged at a ratio 1:5 (U2OS cells) or 1:3 (NIH/3T3 cells) using 0.05% trypsin/ EDTA solution. High-density cells, 0.5 x 10^6/cm^2, were seeded onto the alginate-gelatin printings coated with 120 µM/ml of RGD + 5% EDC + 2.5% NHS diluted in 100 mM $CaCl_2$ for 1 hour [26,27].

Cells growing on alginate-gelatin hydrogel printings were monitored under an inverted phase contrast microscope (Olympus CKX53) and photomicrographs were taken by phase contrast using 10x objective. Images were analyzed by the software ImageJ/FIJI (NIH, USA) [28].

2.2.2. Alginate-gelatin Hydrogel Preparation and Crosslinking

Adapted from Alruwaili *et al* (2019), 2% gelatin (w/v) was added to sterile 0.1 M MES buffer pH 5.5, 6.5, 7.0 or 8.0 + 0.3 M NaCl at 50°C and stirred for 10 minutes. Sodium alginate was then added at a final concentration of 6% (w/v) and stirred thoroughly at 50°C until the hydrogel was homogeneous. The different hydrogel pH values were obtained with the use of MES buffer with different pH values as a solvent. The hydrogel pH was not measured throughout the experiments. Hydrogels were either molded or printed in air or fluid-phase. Hydrogels were then crosslinked overnight with either 5 ml of 100 mM calcium chloride or 5 ml of 100 mM barium chloride both dissolved in deionized water.

2.2.3. Swelling and Degradation Measurement

6% alginate + 2% gelatin pH 5.5, 6.5, 7.0 or 8.0 were molded into 10 mm diameter discs and crosslinked with 5 ml of either 100 mM calcium chloride or 100 mM barium chloride. Hydrogels were weighed before crosslinking (W_0) as a control. To measure the swelling and degradation rate, the hydrogels were also weighed after crosslinking (W_{ACl}), and on day 1 (W_{D1}), day 5 (W_{D5}), day 10 (W_{D10}), day 15 (W_{D15}), day 20 (W_{D20}) and day 25 (W_{D25}) under cell culture conditions incubated with either complete RPMI 1640 or complete DMEM both supplemented with 10% FBS at 37°C with saturating humidity. Hydrogels were air-dried for 30 minutes before having their weight measured. Calculations were made of the percentage of W_0 and experiments were finished when 2/3 of the samples disintegrated.

2.2.4. 3D Printing and Printing Resolution

The extrusion-based NAIAD 3D bioprinter, developed by the 3D Bioprinting Group from the Conway Institute at the University College Dublin, was used to print the alginate-gelatin hydrogel in air and fluid-phase. Briefly, hydrogels were warmed at 37°C for 30 minutes in the bioprinter previously the printing process. Alginate-gelatin printings were obtained using a 0.43 mm ID nozzle gauge 23 under 3 bars of pressure and 1mm/s of speed in air or fluid-phase containing either 100 mM $CaCl_2$ or 100 mM $BaCl_2$. Prior to the fluid-phase printing, six-well plates were treated with 0.1% PEI overnight for hydrogel attachment purposes and washed 3 times with PBS to remove the excess PEI. The width of the strands was measured immediately after printing and analyzed by the software ImageJ/FIJI (NIH, USA) [28].

 doi:10.20944/preprints202309.1086.v1

2.2.5. Cell Viability Assay

LDH Cytotoxicity Detection Kit plus (Roche Diagnostics) was used to quantify U2OS and NIH/3T3 cell death on Day 1 and Day 7 of cell culture. Briefly, cells were incubated for 24 hours with either RPMI 1640 or DMEM each supplemented with 1% FBS, centrifuged, and the amount of LDH on the cell medium was measured at 490 nm by spectrophotometer (SpectraMax M3). Positive and negative controls were done on conventional 2D cell culture on plastic plates. Positive control was treated with 2% Triton X-100 (Sigma Aldrich). Calculations were given as a percentage of control.

2.2.6. Adapted alamarBlue™ Assay

To quantify the metabolic activity of U2OS and NIH/3T3 cells, 10% of alamarBlue™ cell viability reagent (Invitrogen) was added to the DMEM + 10% FBS (NHI/3T3) or RPMI 1640 +10% FBS (U2OS) media on Day 7 of cell culture and incubated for 4 hours. Next, the cell media containing the reduced alamarBlue™ were centrifuged and 100 µl transferred to a 96 well plate. The absorbance of the reduced alamarBlue™ was measured at 570 nm and 600 nm. Calculations were done according to the manufacture's instruction and given as a percentage of control. For calculations purposes, the metabolic activity of cells growing alginate-gelatin hydrogel pH 7.0 crosslinked with 100 mM $CaCl_2$ was considered control (100%).

2.2.7. Statistical Analysis

All statistical data processing was performed using multiple comparison tests on either One-way ANOVA or Two-way ANOVA on GraphPad Prism 9 software. Differences between the groups were considered reliable if $p < 0.05$ and values were expressed as mean ± SD of at least 3 independent experiments.

3. Results

Alginate-gelatin hydrogels were prepared using MES buffer pH of 5.5, 6.5, 7.0 or 8.0 and crosslinked with either 100 mM $CaCl_2$ or 100 mM $BaCl_2$ to study the role of the buffer pH and crosslinking on the hydrogel stability over time. With all other factors remaining the same, addition of different pH buffer is expected to change the pH of the hydrogel, hereafter the substrate's pH. The hydrogels were molded into 10 mm discs and kept under cell culture conditions incubated with either complete RMPI 1640 + 10% FBS or complete DMEM + 10% FBS for 25 days to measure their swelling and degradation rates. As result, we observed that all the conditions presented a weight loss of approximately 50% during the overnight crosslinking with either calcium or barium. However, they regain their initial weight at different speeds. Hydrogels crosslinked with calcium and incubated with RPMI were the least stable under cell culture conditions showing, in general, the fastest degradation rate among all the conditions tested in this work. They regain their initial weight within 24 hours and the swelling of all the hydrogels was between 150 – 200% before degrading (Figure 1A). The crosslinking with calcium and incubation with DMEM showed better stability in comparison to the previous conditions. The swelling of the samples was around 135% before degradation. However, all the substrates, regardless of their pH, degraded within 25 days under cell culture conditions (Figure 1B). The crosslinking with barium provided overall good stability to the alginate-gelatin hydrogel. The incubation with RPMI 1640 showed again to promote higher swelling of the samples (~150%) in comparison to the incubation with DMEM (~120%) (Figure 1C, D). Regarding the hydrogel pH, the hydrogel pH 8.0 presented the weakest stability under cell culture conditions in RPMI regardless of the crosslinking and in DMEM after calcium crosslinking (Figure 1).

Preprints (www.preprints.org) | NOT PEER-REVIEWED | Posted: 15 September 2023 doi:10.20944/preprints202309.1086.v1

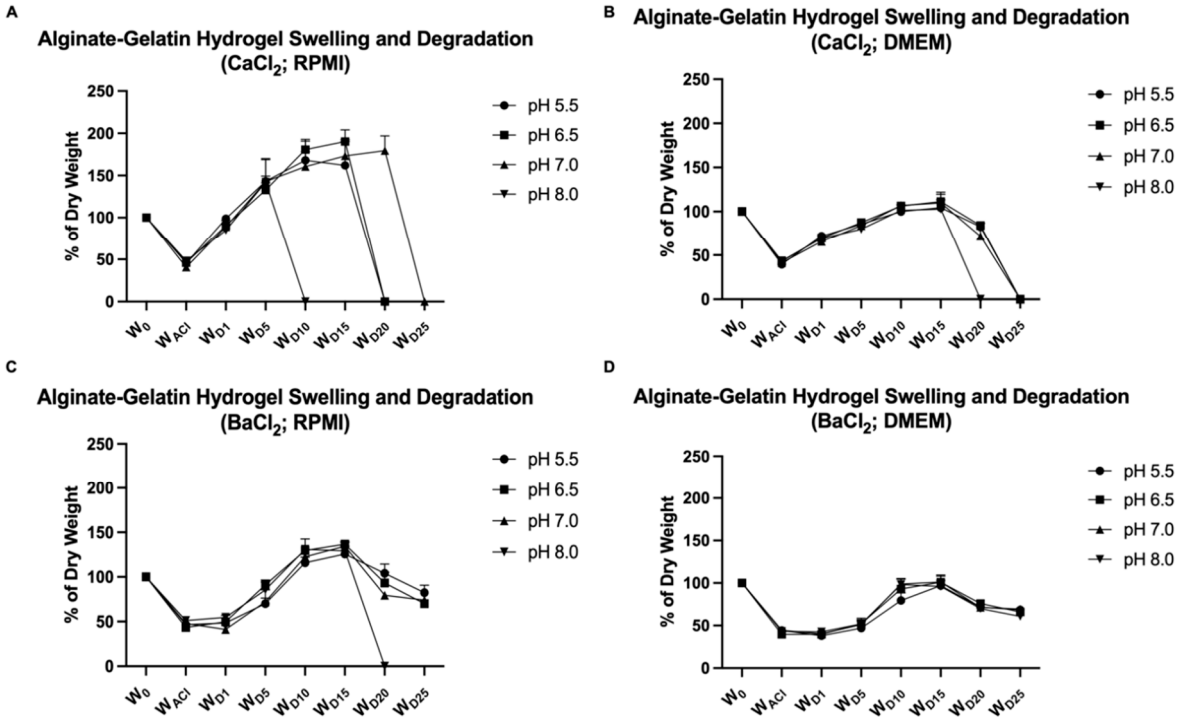

Figure 1. Alginate-gelatin hydrogel swelling and degradation curve. 6% alginate + 2% gelatin hydrogel prepared with 0.1 M MES buffer pH 5.5, 6.5, 7.0 or 8.0 and crosslinked with either 100 mM $CaCl_2$ or 100 mM $BaCl_2$. The samples were kept under cell culture conditions at 37°C with saturating humidity with either RPMI 1640 + 10% FBS or DMEM + 10% FBS. Hydrogels were dried and weighed after moulded into 10 mm diameter discs (W_0= 100%), after crosslinking (W_{Acl}), and on Day 1 (W_{D1}), Day 5 (W_{D5}), Day 10 (W_{D10}), Day 15 (W_{D15}), Day 20 (W_{D20}), and Day 25 (W_{D25}). **(A)** Hydrogels crosslinked with 100 mM $CaCl_2$ and incubated with RPMI 1640 + 10% FBS. **(B)** Hydrogels crosslinked with 100 mM $CaCl_2$ and incubated with DMEM + 10% FBS. **(C)** Hydrogels crosslinked with 100 mM $BaCl_2$ and incubated with RPMI 1640 + 10% FBS. **(D)** Hydrogels crosslinked with 100 mM $BaCl_2$ and incubated with DMEM + 10% FBS. (n= 4, graph of mean ±SD).

Afterwards, alginate-gelatin hydrogels with different pH values had their printability tested under 3 different conditions: air printing, fluid-phase embedding printing with 100 mM $CaCl_2$ support bath, and fluid-phase embedding printing with 100 mM $BaCl_2$ support bath. We have reported in previous findings that to produce printings of the alginate-gelatin hydrogel, the fluid-phase showed to be an efficient way to increase printing fidelity and resolution [28]. To generate the prints, a needle size 0.43 mm ID was used, and the diameter of the strand spread was measured just after printing for the 3 conditions. First, we observed that the spread of the air printing strand was around 200% while both fluid-phase embedding printings restrained the spread of the printed strand as the hydrogel was immediately crosslinked during printing. In addition, the 2 crosslinker solutions used as support bath showed no significant difference on the spread of the strand between them (Figure 2A). The pH of the alginate-gelatin hydrogel had a significant influence on the air printing increasing the spread of the printed strand with the increase of the pH. Whereas both embedding fluid-phase cointainging the crosslinkers only showed a slight increase on the spread of the strand with hydrogel pH 8.0 which was not significant (Figure 2B). The spread of the strand is important for the resolution of the (bio)print and should be calculated and adjusted to obtain the desired printing design. Knowing how the pH of the substrate can influence this aspect and how to overcome it is an important parameter to the biofabrication field. Finally, our results showed that both support bath containing crosslinker (Ca^{2+} and Ba^{2+}) increased the printing fidelity which can be seen especially important at the corners of the prints (Figure 2C).

Preprints (www.preprints.org) | NOT PEER-REVIEWED | Posted: 15 September 2023 doi:10.20944/preprints202309.1086.v1

A

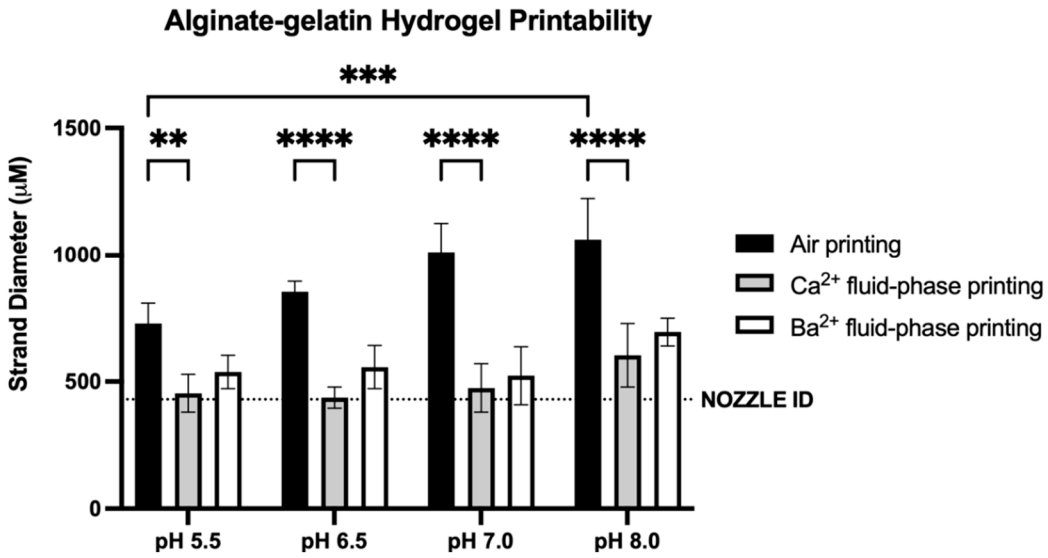

B

	Air printing (pH 5.5 - 8.0)	Ca^{2+} fluid-phase printing (pH 5.5 – 8.0)	Ba^{2+} fluid-phase printing (pH 5.5 – 8.0)
R^2	0.9653	0.6884	0.5081

C

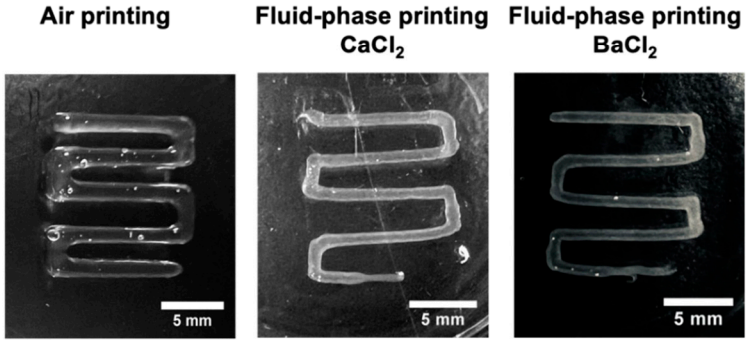

Figure 2. Alginate-gelatin hydrogel printability. **(A)** Quantification of the alginate-gelatin hydrogel pH 5.5, 6.5, 7.0 or 8.0 diameter of the strand printed in air and fluid-phase embedding support bath containing either 100 mM $CaCl_2$ or 100 mM $BaCl_2$. (n= 4, Two-way ANOVA, p**<0.01, p***<0.001, p****<0.0001, ns: not significant). **(B)** R-squared of the effect of increasing pH of alginate-gelatin hydrogel on the spread of the printed line. **(C)** Alginate-gelatin hydrogel pH 7.0 square wave printing obtained under 3 bars and 1mm/s in air and fluid-phase embedding support bath containing either 100 mM $CaCl_2$ or 100 mM $BaCl_2$.

Next, we tested the effect of the crosslinking on the cell viability and metabolic activity of the human osteosarcoma U2OS and the murine fibroblast NIH/3T3. Both cell types are well established in the literature and present high cell proliferative rates which made them good models for this study. The U2OS cells did not show significant difference on the cell death rate of cells growing on alginate-gelatin substrates crosslinked with calcium or barium neither on Day 1 nor on Day 7 of cell culture (Figure 3A). However, the substrate crosslinked with barium led to a 3.62-fold decrease on the U2OS cell metabolic activity in comparison to the substrate crosslinked with calcium (Figure 3B). In a different manner, NIH/3T3 cells presented a high cell death rate on both Day 1 and Day 7 of cell culture on alginate-gelatin hydrogel crosslinked with barium, 45% and 60% respectively, in comparison to 10% and 20%, respectively, of cell death rate on the same hydrogel crosslinked with calcium (Figure 3C). Moreover, NIH/3T3 cells also showed less metabolic activity on the substrate

Preprints (www.preprints.org) | NOT PEER-REVIEWED | Posted: 15 September 2023 doi:10.20944/preprints202309.1086.v1

crosslinked with barium (83.91%) in comparison to the one crosslinked with calcium (100%) (Figure 3D). Even though the crosslinking with barium showed better stability to the alginate-gelatin hydrogel, the 2 cell types studied in this work did not show good cell viability and/or cell metabolic activity on substrates crosslinked with Ba^{2+}.

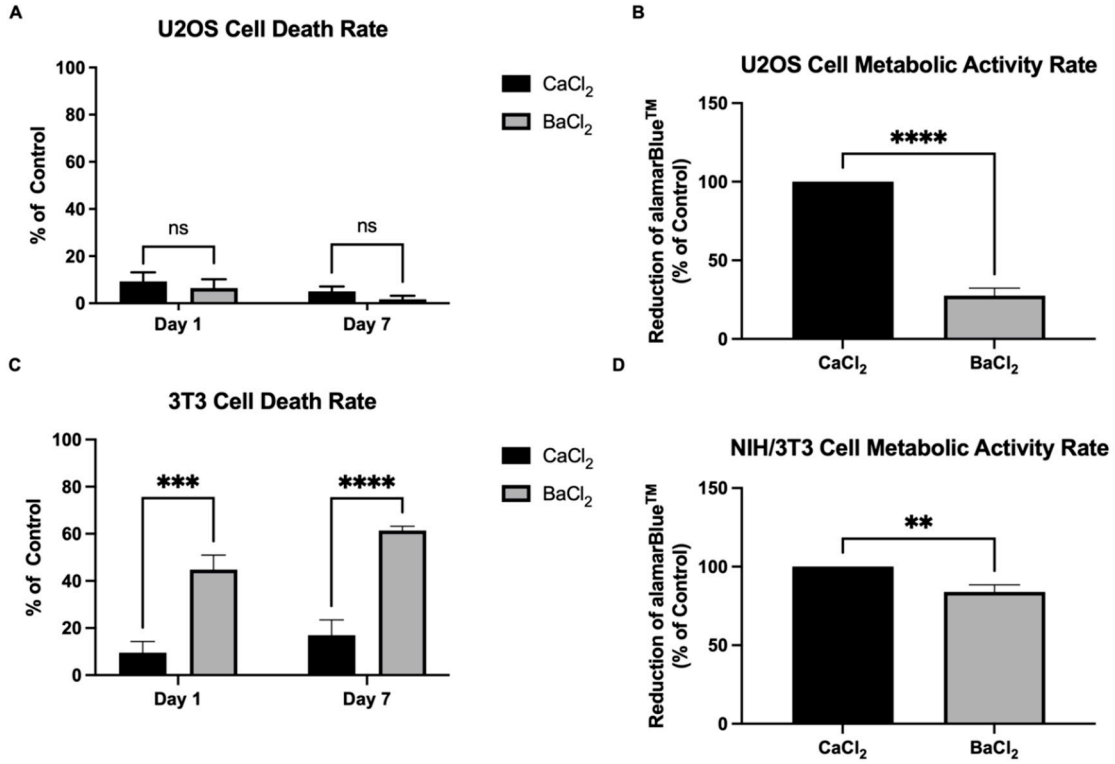

Figure 3. (A) LDH Cytotoxicity Assay of U2OS cells on alginate-gelatin hydrogel pH 7.0 crosslinked with either 100 mM $CaCl_2$ or 100 mM $BaCl_2$ on Days 1 and 7 of cell culture (day 1 n= 4 and day 7 n= 3, Two-way ANOVA, ns: not significant). **(B)** U2OS metabolic activity rate quantified by the % of alamarBlue™ reduction on Day 7 of cell culture on alginate-gelatin hydrogel pH 7.0 crosslinked with either 100 mM $CaCl_2$ or 100 mM $BaCl_2$ (n= 4, Two-way ANOVA, p****< 0.0001). **(C)** LDH Cytotoxicity Assay of NIH/3T3 cells on alginate-gelatin hydrogel pH 7.0 crosslinked with either 100 mM $CaCl_2$ or 100 mM $BaCl_2$ on days 1 and 7 of cell culture (n= 3, Two-way ANOVA, p***< 0.001, p****< 0.0001). **(D)** NIH/3T3 metabolic activity rate quantified by the % of alamarBlue™ reduction on Day 7 of cell culture on alginate-gelatin hydrogel pH 7.0 crosslinked with either 100 mM $CaCl_2$ or 100 mM $BaCl_2$ (n= 4, Two-way ANOVA, p**< 0.01).

To study the effect of the substrate pH on cell viability and metabolic activity, U2OS and NIH/3T3 were seeded onto alginate-gelatin prepared with MES buffer of pH 5.5, 6.5, 7.0, and 8.0. Cells were kept in culture for 7 days incubated with complete RPMI +10% FBS (U2OS) or complete DMEM + 10% FBS (NHI/3T3). Our results showed that U2OS cells growing on alginate-gelatin hydrogels prepared with different pH values presented a good cell viability of approximately 90% of viable cells on Day 1 and Day 7 of cell culture. Some cell protective effect was observed by the substrate at pH 7.0, however no significant difference on cell viability was caused by the substrate pH (Figure 4A). On the contrary, the substrate presenting different pH values led to a significant difference on the cell metabolic activity. Cells growing on substrates prepared with pH 7.0 and 8.0 showed an important increase on the cell metabolism in comparison to cells growing on acidic substrates after 7 days of cell culture. An increase of 2.25 fold was observed on the cell metabolism of cells on substrate pH 8.0 in comparison to cells on the substrate pH 5.5. Even though all the cells were grown in RPMI 1640 cell culture medium under physiological pH. This result shows that it is possible to grow cells over the influence of the pH of interest by preparing a substrate with a specific pH independent of the cell culture medium utilized. In the same way, the NIH/3T3 cells also showed good viability of the cells regardless of the substrate pH values on Day 1 and Day 7 of cell culture

Preprints (www.preprints.org) | NOT PEER-REVIEWED | Posted: 15 September 2023 doi:10.20944/preprints202309.1086.v1

(Figure 4C). However, in the same fashion as U2OS cells, NIH/3T3 also showed significant difference on the cell metabolism due to the substrate pH. NIH/3T3 cells growing on substrate pH 7.0 presented higher metabolic activity in comparison to cells growing on substrates pH 6.5 and 8.0 and even greater cell metabolic activity in comparison to cells growing on substrates pH 5.5 (Figure 4D).

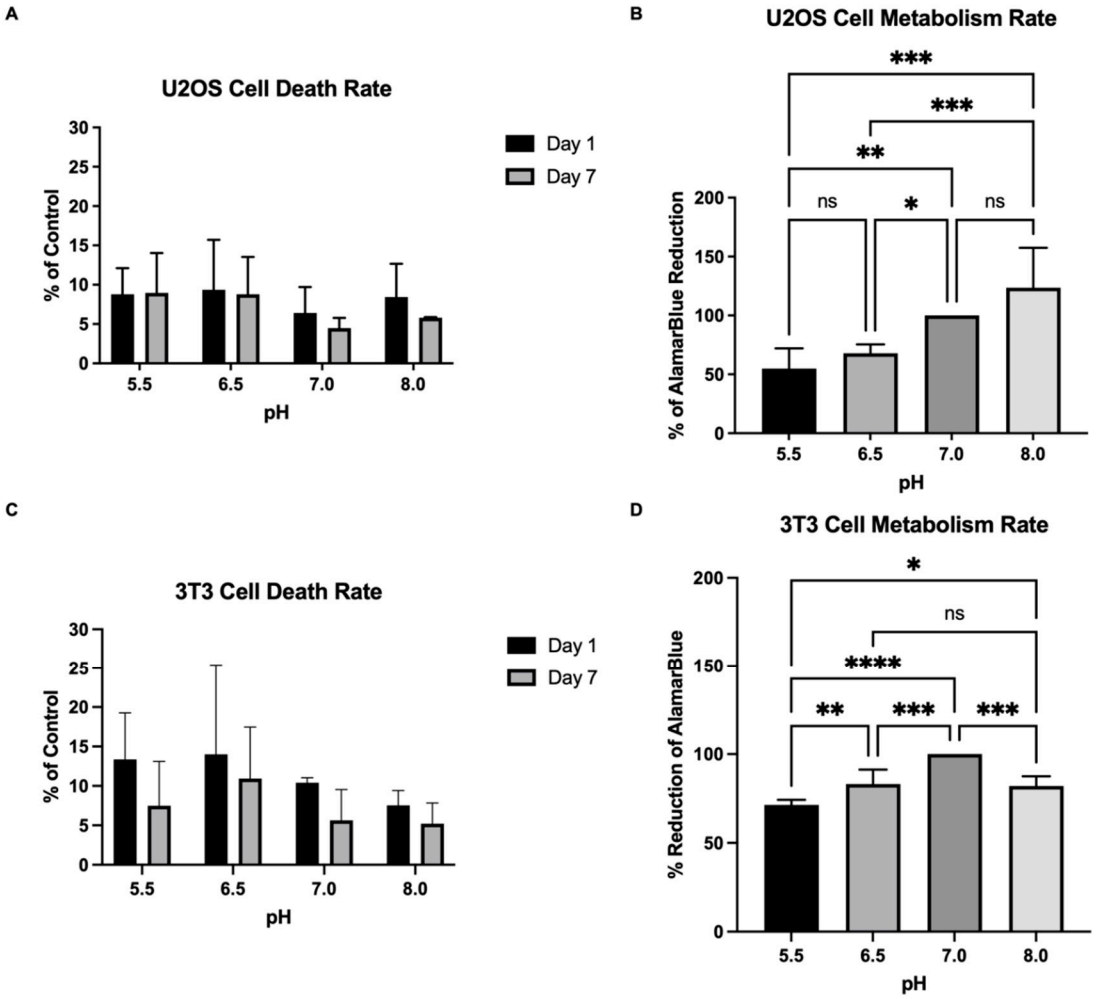

Figure 4. (A) LDH Cytotoxicity assay of U2OS cells on alginate-gelatin hydrogel pH 5.5, 6.5, 7.0, and 8.0 on Days 1 and 7 of cell culture (day 1 n= 4 and day 7 n= 3, Two-way ANOVA, not significant). **(B)** U2OS metabolic activity rate quantified by the % of alamarBlue™ reduction on Day 7 of cell culture on alginate-gelatin hydrogel pH 5.5, 6.5, 7.0, and 8.0 (n= 6, Two-way ANOVA, p*<0.05, p**<0.01, p***< 0.001, ns: not significant). **(C)** LDH Cytotoxicity assay of NIH/3T3 cells on alginate-gelatin hydrogel pH 5.5, 6.5, 7.0, and 8.0 on Days 1 and 7 of cell culture (Day 1 n= 3 and Day 7 n= 3, Two-way ANOVA, not significant). **(B)** NIH/3T3 metabolic activity rate quantified by the % of alamarBlue™ reduction on day 7 of cell culture on alginate-gelatin hydrogel pH 5.5, 6.5, 7.0, and 8.0 (n= 6, Two-way ANOVA, p*<0.05, p**<0.01, p***< 0.001, p****< 0.0001, ns: not significant).

Finally, we observed that the pH of the substrate also influences the cell-cell and cell-matrix interactions, with cells favouring interactions with each other below pH 7 and the matrix at pH 7 and above. Alginate-gelatin substrates at pH 5.5 and 6.5 led to the formation of cell aggregates, whereas substrates at pH 7.0 and 8.0 showed cells growing more spread out after 7 days of cell culture (Figure 5).

Preprints (www.preprints.org) | NOT PEER-REVIEWED | Posted: 15 September 2023 doi:10.20944/preprints202309.1086.v1

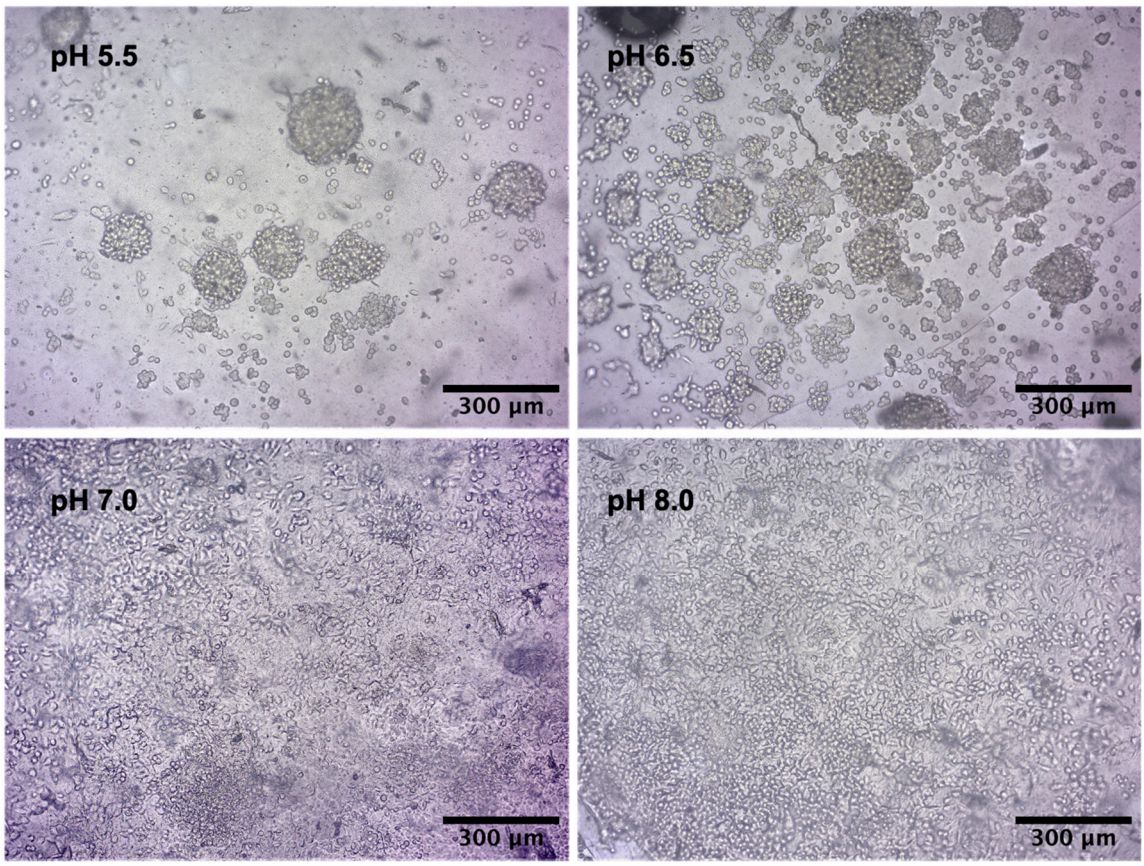

Figure 5. Light microscopy images of U2OS cell culture on alginate-gelatin hydrogel pH 5.5, 6.5, 7.0, and 8.0 on Day 7 of cell culture. Magnification of 10x.

4. Discussion

Alginate hydrogels can be crosslinked with many divalent cations. In the present study we tested the swelling and degradation rates of alginate-gelatin hydrogels with different pH values after crosslink with either 100 mM $CaCl_2$ or 100 mM $BaCl_2$. Both cations are widely used in the biofabrication field to crosslink alginate for different purposes such as drug encapsulation and delivery, wound dressing, tissue formation, etc. Besides, the choice of the crosslinker and its concentration can tailor some of the hydrogel mechanical properties like elasticity, strength, stiffness, swelling, etc [30]. Haper and Barbut (2014) showed that alginate films crosslinked with $BaCl_2$ had the highest tensile strength and Young's modulus among Ba^{2+}, Ca^{2+}, Mg^{2+}, Sr^{2+}, and Zn^{2+} while films crosslinked with $CaCl_2$ had the highest puncture strength [18]. Alginate's affinity to divalent cations was shown to decrease with the order: $Pb^{2+} > Cu^{2+} > Cd^{2+} > Ba^{2+} > Sr^{2+} > Ca^{2+} > Co^{2+}$, Ni^{2+}, $Zn^{2+} > Mn^{2+}$ [31,32] and gel strength decreases with decreasing affinity. Our study is in accordance with the literature as barium crosslinking provided better stability for all the tested hydrogels in comparison to calcium crosslinking. Additionally, we observed a shrinkage of approximately 50% on all hydrogels incubated with both crosslinker solutions ($CaCl_2$ and $BaCl_2$) for 24h. Saitoh *et al* has described a similar effect of alginate hydrogel crosslinked with Ca^{2+} and incubated with increasing concentrations of $CaCl_2$ which showed increasing shrinkage rate. Increasing the binding between Ca^{2+} and alginate residual carboxylate groups leads to the increase of the crosslinking degree which facilitates the gel shrinkage [33]. In the present study we show that Ba^{2+} presents similar effect to Ca^{2+} regarding the alginate hydrogel shrinkage extent after overnight incubation. Besides the crosslinker effect on the hydrogel, we also showed that the cell culture medium in which the hydrogel is kept also plays an important role as hydrogels incubated with complete DMEM + 10% FBS presented overall better stability over time in comparison to the same hydrogels incubated with complete RPMI 1640 + 10% FBS. Even though both media had the same physiological pH. In addition, among the hydrogels presenting different pH values, the hydrogel at pH 8.0 showed the weakest strength under

 doi:10.20944/preprints202309.1086.v1

cell culture conditions in general degrading faster than the hydrogels at pH 5.5, 6.5, and 7.0. Anionic hydrogels such as alginate swell at high pH and shrink at lower pH. The deprotonation of the carboxylic groups of the alginate molecules at high pH decrease the strength of the hydrogel as the negatively charged ions repels each other leading to the hydrogel swelling and fast degradation. In an opposite fashion, acidic media lead to the protonation of alginate carboxylic groups decreasing repulsion and causing the shrinkage because of water loss [34–36]. In this study we showed that we can also tailor the alginate hydrogel swelling and degradation/dissociation rates by changing the pH of the solvent used to produce the hydrogel independently of the medium's pH.

This pH effect was also seen on the printability of the hydrogel as the spread of the strand significantly increased with the increase of the hydrogel pH when printing in air. However, the fluid-phase embedding printing using either 100 mM $CaCl_2$ or 100 mM $BaCl_2$ as support baths showed to be efficient to prevent spreading from happening. The slight increase on the spreading of the line of hydrogel pH 8.0 printed in fluid-phase was not significant as the immediate crosslink after printing the hydrogel was sufficient to keep its shape. No significant difference was seen between calcium and barium in relation to the printability of the hydrogel with different pH values. Although, barium support bath showed lower correlation between the spread of the strand and the increasing pH of the hydrogel in comparison to calcium. Jui-Jung *et al* (2017) has described that barium crosslinking bath with different pH values does not influence alginate particles shape while the crosslinking with calcium at lower pH values does [37].

However, even though the crosslinking with barium provided more stability and strength to the alginate-gelatin hydrogel, both U2OS and NIH/3T3 cells showed significantly higher cell metabolic activity on hydrogels crosslinked with calcium in comparison to the hydrogels crosslinked with barium. It was described that both crosslinkers, Ca^{2+} and Ba^{2+}, present a rate of release of molecules to the medium due to their relatively weak ionic interaction and competition with other cations present in the medium. Chan and Mooney (2013) described that alginate crosslinked with calcium releases around 43% of the Ca^{2+} incorporated in its meshes within the first 10 hours of incubation with cell culture medium and keep releasing Ca^{2+} molecules at a lower rate throughout time as Ca^{2+} is slowly exchanged by sodium cations present in the cell culture medium [17]. While Ba^{2+} also presented a high release rate from alginate *in vitro* and *in vivo* that might be of safety concern [38]. In addition, it is widely known that Ca^{2+} is one of the most important intracellular second messenger participating in an extensive number of cell signalling pathways related to cell adhesion, proliferation, metabolism, apoptosis, etc [39]. There is a possibility that Ba^{2+} ions released from alginate can be competing to Ca^{2+} in important metabolic pathways decreasing the metabolic rate of cells seeded onto substrate crosslinked with Ba^{2+} [40–42]. However, there are few studies over the effect of barium crosslinking on cell activity and metabolism and further investigations should be done for better understanding. We also observed that Ba^{2+} crosslinking did not increase cell death in comparison to Ca^{2+} crosslinking on U2OS cells, whereas Ba^{2+} crosslinking increased the NIH/3T3 cell death rate significantly.

To study the influence of the substrate pH on cell viability and metabolism, U2OS and NIH/3T3 cells were seeded onto substrates with different pH values. Bone cells respond to even slight differences on the environment pH having higher osteoclast activity in acidic pH while osteoblasts have higher activity in basic pH [43–45]. This is one of the homeostatic mechanisms to keep the systemic acid-base balance. Matsubara *et al* (2013) showed that U2OS cells modulate their proliferation rate in response to the extracellular pH increasing proliferation in higher pH values [46]. In this work we used the same cell type to investigate if by changing the substrate pH would change cell behaviour. Our results showed that different substrate pH led to a significant difference of cell metabolism and no influence on the cell viability. Corroborating the literature, osteoblasts growing on basic substrate showed greater cell metabolic activity in comparison to cells growing on acidic substrates. Our results, however, showed that independently of the cell culture medium pH, the substrate's pH played a crucial role on cell behaviour. Besides, we observed that the U2OS cells can modulate the cell arrangement in response to the substrate pH forming aggregates on acidic printings and spready growth on basic printings. Cells start to grow in 3D aggregates when the environment

is unfavourable to cell-substrate interactions and lead cells to cell-cell and cell-ECM interactions instead [47].

Studying the interstitial pH of each tissue is a difficult task. There is no available data for human bone tissue. However, mice embryos were reported to have no impairment on their development in pH between 7.17 and 7.37 [48]. In this work we used the NHI/3T3 cells which are murine embryonic fibroblasts. It is not reported from which tissue it is originated, but Dastagir *et al* (2014) showed that this cell type can differentiate into adipogenic, chondrogenic, and osteogenic lineages [49]. Our result showed that NHI/3T3 cells had a higher metabolic activity on substrates prepared with a buffer of pH 7.0 in comparison to substrates prepared with pH 5.5, 6.5, and 8.0 even though all the cells were kept In cell culture medium under physiological pH. In addition, the pH of the buffer also did not influence the NHI/3T3 cell viability. Future work in this direction should attempt to directly measure substrate pH as a function of time.

5. Conclusion

The bioengineering field is a very complex area of science because it involves several steps which are all very specific to each cell type and circumstance. In this study we aimed to understand the importance of carefully studying the pH of 3D prints. In addition, we also aimed to understand how crosslinking affects not only the mechanical properties of the hydrogels, but also influences cell viability, growth, and behaviour on the prints. In essence, our findings showed that the pH of the microenvironment in which the cells are in direct contact to grow influences the cell behaviour independently of the pH of the cell culture medium in the range studied. Moreover, barium crosslinking provided better stability to alginate-gelatin hydrogels independently of the substrate pH. However, U2OS and NIH/3T3 cells showed significantly less metabolic activity when grown on substrates crosslinked with Ba^{2+} in comparison to Ca^{2+} crosslinking. Besides, Ba^{2+} crosslinking increased NIH/3T3 cell death. Therefore, Ca^{2+} showed to be a better crosslinking for growing both U2OS and NIH/3T3 cells on alginate-gelatin hydrogels. This illustrates that each cell type can respond differently to different substrate pH values and crosslinking protocols which shows the importance of adjusting the conditions in 3D printing to achieve desired results.

Conflicts of Interest: The authors declare no conflict of interest.

References

1. Derr K, Zou J, Luo K, Song MJ, Sittampalam GS, Zhou C, Michael S, Ferrer M, Derr P. Fully Three-Dimensional Bioprinted Skin Equivalent Constructs with Validated Morphology and Barrier Function. Tissue Eng Part C Methods. 2019 Jun;25(6):334-343. doi: 10.1089/ten.TEC.2018.0318.
2. Diloksumpan P, de Ruijter M, Castilho M, Gbureck U, Vermonden T, van Weeren PR, Malda J, Levato R. Combining multi-scale 3D printing technologies to engineer reinforced hydrogel-ceramic interfaces. Biofabrication. 2020 Feb 19;12(2):025014. doi: 10.1088/1758-5090/ab69d9.
3. Lv S, Nie J, Gao Q, Xie C, Zhou L, Qiu J, Fu J, Zhao X, He Y. Micro/nanofabrication of brittle hydrogels using 3D printed soft ultrafine fiber molds for damage-free demolding. Biofabrication. 2020 Feb 19;12(2):025015. doi: 10.1088/1758-5090/ab57d8.
4. Weisgrab G, Guillaume O, Guo Z, Heimel P, Slezak P, Poot A, Grijpma D, Ovsianikov A. 3D Printing of large-scale and highly porous biodegradable tissue engineering scaffolds from poly(trimethylene-carbonate) using two-photon-polymerization. Biofabrication. 2020 Oct 1;12(4):045036. doi: 10.1088/1758-5090/abb539.
5. Huang NF, Li S. Regulation of the Matrix microenvironment for stem cell engineering and regenerative medicine. Annals of Biomedical Engineering. Apr (2011) 39:1201–1214.
6. Di Giuseppe M, Law N, Webb B, Macrae AR, Liew JL, Sercombe BT, Dilley JR, Doyle JB. Mechanical behaviour of alginate-gelatin hydrogels for 3D bioprinting. Journal of the Mechanical Behavior of Biomedical Materials 79 (2018) 150-157.
7. Jiang T, Munguia-Lopez GJ, Gu K, Bavoux MM, Flores-Torres S, Kort-Mascort J, Grant J, Vijayakumar S, Leon-Rodriguez DA, Ehrlicher JA, Kinsella MJ. Engineering bioprintable alginate/gelatin composite hydrogels with tunable mechanical and cell adhesive properties to modulate tumor spheroid growth kinetics. Biofabrication (2019) Dec 31;12(1):015024.

8. Mondal A, Gebeyehu A, Miranda M, Bahadur D, Patel N, Ramakrishnan S, Rishi KA, Singh M. Characterization and printability of sodium alginate -gelatin hydrogel for bioprinting NSCLC co-culture. Scientific Reports (2019) 9:19914.
9. Alsberg E, Anderson KW, Albeiruti A, Franceschi RT, Mooney DJ. Cell interactive alginate hydrogels for bone tissue engineering. J Dent Res (2001) 80: 2025–9.
10. Pan T, Song W, Cao X, Wang Y. 3D bioplotting of gelatin/alginate scaffolds for tissue engineering: influence of crosslinking degree and pore architecture on physicochemical properties. Journal of Materials Science & Technology (2016) 32, 889–900.
11. Lee KY, Rowley JA, Eiselt P, Moy EM, Bouhadir KH, Mooney DJ. Controlling mechanical and swelling properties of alginate hydrogels independently by cross-linker type and crosslinking density. Macromolecules. 2000; 33:4291–4294.
12. Liu J, Su C, Chen Y, Tian S, Lu C, Huang W, Lv Q. Current Understanding of the Applications of Photocrosslinked Hydrogels in Biomedical Engineering. Gels. 2022 Apr 1;8(4):216. doi: 10.3390/gels8040216.
13. Hennink WE, van Nostrum CF. Novel crosslinking methods to design hydrogels. Adv. Drug Deliv. Rev. 2012;64:223–236. doi: 10.1016/j.addr.2012.09.009.
14. Zhao XH, Huebsch N, Mooney DJ, Suo ZG. Stress-relaxation behavior in gels with ionic and covalent crosslinks. J Appl Phys. 2010; 107 063509/1–5.
15. Lee YK, Mooney JD. Alginate: properties and biomedical applications. Progress in Polymer Science 37 (2012) 106–126.
16. Grant GT, Morris ER, Rees DA, Smith PJC, Thom D. Biological interactions between polysaccharides and divalent cations–- egg-box model. FEBS Lett. 1973; 32:195–198.
17. Chan G, Mooney DJ. Ca(2+) released from calcium alginate gels can promote inflammatory responses *in vitro* and *in vivo*. Acta Biomater. 2013 Dec;9(12):9281-91. doi: 10.1016/j.actbio.2013.08.002. Epub 2013 Aug 9.
18. Harper, B.A.; Barbut, S.; Lim, L.T.; Marcone, M.F. Effect of Various Gelling Cations on the Physical Properties of "Wet" Alginate Films. J. Food Sci. 2014, 79, E562–E567.
19. Luca G, Calvitti M, Nastruzzi C, Bilancetti L, Becchetti E, Angeletti G, Mancuso F, Calafiore R. Encapsulation, *in vitro* characterization, and *in vivo* biocompatibility of Sertoli cells in alginate-based microcapsules. Tissue Eng. 2007 Ma r;13(3):641-8. do i: 10.1089/ten.2006.0137.
20. Mores L, França EL, Silva NA, Suchara EA, Honorio-França AC. Nanoparticles of barium induce apoptosis in human phagocytes. Int J Nanomedicine. 2015 Sep 28;10:6021-6. doi: 10.2147/IJN.S90382.
21. FitzSimons TM, Anslyn EV, Rosales AM. Effect of pH on the Properties of Hydrogels Cross-Linked via Dynamic Thia-Michael Addition Bonds. ACS Polym Au. 2022 Apr 13;2(2):129-136. doi: 10.1021/acspolymersau.1c00049.
22. Kolotova DS, Borovinskaya EV, Bordiyan VV, Zuev YF, Salnikov VV, Zueva OS, Derkach SR. Phase Behavior of Aqueous Mixtures of Sodium Alginate with Fish Gelatin: Effects of pH and Ionic Strength. Polymers (Basel). 2023 May 10;15(10):2253. doi: 10.3390/polym15102253.
23. Bouhadir KH, Lee KY, Alsberg E, Damm KL, Anderson KW, Mooney DJ. Degradation of partially oxidized alginate and its potential application for tissue engineering. Biotechnol Prog. 2001 Sep-Oct;17(5):945-50. doi: 10.1021/bp010070p.
24. Wu X, Lin M, Li Y, Zhao X, Yan F. Effects of DMEM and RPMI 1640 on the biological behavior of dog periosteum-derived cells. Cytotechnology. 2009 Mar;59(2):103-11. doi: 10.1007/s10616-009-9200-5.
25. Thomas JH, Quentin J, Rachelle NP, Joon HP, Martin SG, Hao-Jan S, Mohamed HR, Andrew RH, Adam WF. Three-dimensional printing of complex biological structures by freeform reversible embedding of suspended hydrogels. Sci. Adv. (2015);1:e1500758.
26. Rowley JA, Madlambayan G, Mooney DJ. Alginate hydrogels as synthetic extracellular matrix materials. Biomaterials. (1999) Jan;20(1):45-53.
27. Souza A, McCarthy K, Rodriguez BJ, Reynaud EG. The Use of Fluid-phase 3D Printing to Pattern Alginate-gelatin Hydrogel Properties to Guide Cell Growth and Behaviour In Vitro. bioRxiv 2023.07.08.547691; doi: https://doi.org/10.1101/2023.07.08.547691.
28. Schindelin J, Arganda-Carreras I, Frise E, Kaynig V, Longair M, Pietzsch T, Preibisch S, Rueden C, Saalfeld S, Schmid B, *et al*. Fiji: an open-source platform for biological-image analysis. Nat Methods. (2012); 9(7):676–82.
29. Alruwaili M, Lopez JA, McCarthy K, Reynaud EG, Rodriguez BJ. Liquid-phase 3D bioprinting of gelatin alginate hydrogels: influence of printing parameters on hydrogel line width and layer height. Bio-des. Manuf. 2, 172–180 (2019).
30. Tan J, Luo Y, Guo Y, Zhou Y, Liao X, Li D, Lai X, Liu Y. Development of alginate-based hydrogels: Crosslinking strategies and biomedical applications. Int J Biol Macromol. 2023 Jun 1;239:124275. doi: 10.1016/j.ijbiomac.2023.124275.
31. Haug A. The affinity of some divalent metals to different types of alginates. Acta Chem. Scand. 1961; 15:1794–1795.

32. Haug A, Smidsrød O. Selectivity of some anionic polymers for divalent metal ions. Acta Chem. Scand. 1970; 24:843–854.
33. Saitoh S, Araki Y, Kon R, Katsura H, Taira M. Swelling/deswelling mechanism of calcium alginate gel in aqueous solutions. Dent Mater J. 2000 Dec;19(4):396-404. doi: 10.4012/dmj.19.396.
34. Xiangning S, Yudong Z, Guojie W, Qinghua L, Jinsheng F. pH- and electro-response characteristics of bacterial cellulose nanofiber/sodium alginate hybrid hydrogels for dual controlled drug delivery. RSC Adv., 2014, 4, 47056–47065. doi: 10.1039/c4ra09640a.
35. George M, Abraham TE. pH sensitive alginate-guar gum hydrogel for the controlled delivery of protein drugs. Int J Pharm. 2007 20;335(1-2):123-129. doi: 10.1016/j.ijpharm.2006.11.009.
36. Tezar R, Su HC, Sangeeta P, Bhesh B. Time dependent gelling properties of cuboid alginate gels made by external gelation method: Effects of alginate-CaCl2 solution ratios and pH. Food Hydrocolloids. 2019 (90):232-240. doi:10.1016/j.foodhyd.2018.12.022.
37. Jui-Jung C, Yu-Ya H, Szu-Hsuan L, Tzu-Fang H, Wen-Ying H, Shu-Ling H, Yung-Sheng L. Effects of pH on the Shape of Alginate Particles and Its Release Behavior. International Journal of Polymer Science. 2017. Article ID 3902704, 9 pages.
38. Mørch YA, Qi M, Gundersen PO, Formo K, Lacik I, Skjåk-Braek G, Oberholzer J, Strand BL. Binding and leakage of barium in alginate microbeads. J Biomed Mater Res A. 2012 Nov;100(11):2939-47. doi: 10.1002/jbm.a.34237.
39. Clapham, D. E. Calcium signaling. Cell (2007) 131:1047–58.
40. Przywara DA, Chowdhury PS, Bhave SV, Wakade TD, Wakade AR. Barium-induced exocytosis is due to internal calcium release and block of calcium efflux. Proc Natl Acad Sci U S A. 1993 Jan 15;90(2):557-61. Doi: 10.1073/pnas.90.2.557.
41. Heldman E, Levine M, Raveh L, Pollard HB. Barium ions enter chromaffin cells via voltage-dependent calcium channels and induce secretion by a mechanism independent of calcium. J Biol Chem. 1989 May 15;264(14):7914-20.
42. Gilmore RS, Bullock CG, Sanderson G, Wallace WF. Ultrastructural evidence in rabbit ear arteries that barium enters smooth muscle cells through calcium channels. Q J Exp Physiol. 1986 Jul;71(3):417-22. doi: 10.1113/expphysiol.1986.sp003000.
43. Sprague SM, Krieger NS, Bushinsky DA. Greater inhibition of *in vitro* bone mineralization with metabolic than respiratory acidosis. Kidney Int. 1994 Oct;46(4):1199-206. doi: 10.1038/ki.1994.385. PMID: 7861717.
44. Brandao-Burch A, Utting JC, Orriss IR, Arnett TR. Acidosis inhibits bone formation by osteoblasts in vitro by preventing mineralization. Calcif Tissue Int. 2005 Sep;77(3):167-74. doi: 10.1007/s00223-004-0285-8.
45. Arnett TR. Extracellular pH regulates bone cell function. J Nutr. 2008 Feb;138(2):415S-418S. doi: 10.1093/jn/138.2.415S.
46. Matsubara T, Diresta GR, Kakunaga S, Li D, Healey JH. Additive Influence of Extracellular pH, Oxygen Tension, and Pressure on Invasiveness and Survival of Human Osteosarcoma Cells. Front Oncol. 2013 Jul 29;3:199. doi: 10.3389/fonc.2013.00199.
47. Białkowska K, Komorowski P, Bryszewska M, Miłowska K. Spheroids as a Type of Three-Dimensional Cell Cultures-Examples of Methods of Preparation and the Most Important Application. Int J Mol Sci. 2020 Aug 28;21(17):6225. Doi: 10.3390/ijms21176225.
48. John DP, Kiessling AA. Improved pronuclear mouse embryo development over an extended pH range in Ham's F-10 medium without protein. Fertil Steril. 1988 Jan;49(1):150-5. doi: 10.1016/s0015-0282(16)59667-8.
49. Dastagir K, Reimers K, Lazaridis A, Jahn S, Maurer V, Strauß S, Dastagir N, Radtke C, Kampmann A, Bucan V, Vogt PM. Murine embryonic fibroblast cell lines differentiate into three mesenchymal lineages to different extents: new models to investigate differentiation processes. Cell Reprogram. 2014 Aug;16(4):241-52. doi: 10.1089/cell.2014.0005.